Structure and energetics of Ni, Ag, and Au nanoclusters

K. Michaelian, N. Rendón, and I. L. Garzón
Instituto de Física, Universidad Nacional Autónoma de México, Apartado Postal 20-364, 01000 Mexico D.F., Mexico
(Received 28 January 1999; revised manuscript received 17 March 1999)

The geometries and binding energies of the most stable isomers of nickel, silver, and gold nanoclusters of size 6, 7, 12, 13, 14, 19, 38, 55, and 75 atoms, predicted with an *n*-body Gupta potential, are presented. An exhaustive search for low-energy minima on the potential energy surface was carried out using an evolutive (genetic-symbiotic) algorithm. Our results confirm the existence of *disordered* global minima for gold clusters of 19, 38, and 55 atoms in size, and disordered low-energy isomers for the 75-atom gold cluster. Disordered structures are also isomers of nickel and silver clusters but they are not among the global minima of these metals. Comparison of the structure factors of the disordered and ordered isomers of gold with published experimental x-ray powder diffraction data suggests that the disordered structures are real. The relation between the form of the *n*-body potential and the structure of the global minimum is studied, leading to an explanation of why these disordered states were located with the Gupta potential but not with certain other models of the metal bonding. [S0163-1829(99)05524-1]

I. INTRODUCTION

Metal nanoclusters containing fewer than ~400 atoms show quantum size effects[1] which give them unique properties and make them interesting candidates for the building blocks of nanostructured materials and nanoelectronic digital circuits.[2–4] Before such practical applications can be developed, however, the cluster's chemical, thermodynamic, electronic, and optical properties must be delineated. This in turn requires a complete and unambiguous characterization of the cluster's geometrical structure. Recent experiments have been able to grow, and separate in mass, gold clusters down to sizes as small as ~1 nm in diameter (~38 atoms).[1,5] This recent improvement in experimental isolation capability to smaller sizes has allowed direct comparison of experimental geometries with theoretical predictions based on unbiased and exhaustive searches for the low-energy minima of clusters using model potentials[6,7] and refined with first principles calculations.[6]

X-ray powder diffraction studies of Au nanoclusters of ~38, 75, 101, 146, 200, 225, and 459 atoms in size, and grown with passivating agents, have been interpreted as revealing cores which are ordered; of the fcc truncated octahedral motif for the 38-, 225-, and 459-atom clusters and of the truncated decahedral motif for the rest.[1,5,8] However, calculations using the *n*-body Gupta potential and corroborated through density functional theory[6,9,10] (DFT) in the local density approximation (LDA) indicate that isolated gold clusters between ~38 and 75 atoms in size have disordered global minima, with pair distribution functions which show little regularity in the geometry, even at the so-called ''magic'' cluster numbers of 38, 55, and 75 atoms. These geometries, in fact, remain as the lowest free energy states at the finite temperatures of the experimental works.[6,10] Disordered ground state structures have also been reported for Pt_{13} using DFT (Ref. 11) and for Pt_{55} using an embedded-atom model (EAM) potential.[12] On the other hand, other searches using embedded-atom potentials[5] and the Sutton-Chen potential[7] report ordered (crystalline and quasicrystalline) global minima.

One of the factors contributing to this controversy is the complexity of the potential energy surfaces of Au clusters. The short range of the Au potential leads to a very large number of local minima, making localization of the true global minimum extremely difficult. Since the number of local minima in the potential energy surface increases rapidly, probably exponentially, with size, this uncertainty becomes even worse for larger clusters. Also, different potential models of the metal bond yield different energy orderings for the lowest-energy isomers. The experimental conclusions reported above, for example, were based on a comparison of the experimental structure factors with simulated equivalents of a rather limited set of mainly low-energy ordered structures which did not include the disordered structures reported here.

The objectives of this article were first to locate the global minimum and an extensive set of stable low-energy isomers of each cluster, and second, to study the effect of the form of the potential on the geometrical structure and energy ordering of the isomers. The first objective was addressed by making exhaustive global searches on the potential energy surface. This paper presents the predictions for the structure and energy of the lowest-energy isomers of Au, Ag, and Ni of size 6, 7, 12, 13, 14, 19, 38, 55, and 75 atoms, as given by the *n*-body Gupta potential. Fifty thousand random initial configurations were globally optimized for the sizes 6–38, and 80 000 for the 55- and 75-atom clusters. The search was performed with a symbiotic algorithm,[13] a variant of the genetic algorithm, and then followed with a conjugate gradient local optimization.

Concerning the second objective relating potential form, energy ordering, and geometrical structure, it is known, for example, that the lowest-energy structures and thermodynamics of clusters modeled with potentials depend sensitively on both the attractive range and the repulsive core.[14–17] Furthermore, it is known that *n*-body effects are important for metal clusters[18] and since different potentials

TABLE I. Parameters of the Gupta potential used in this work. p and q were obtained from Ref. 20. A was obtained by minimizing the bulk fcc energy.

	A	p	q
Ni	0.08499	10.00	2.70
Ag	0.09944	10.12	3.37
Au	0.11844	10.15	4.13

treat this part differently, this could lead to global minima of different structure. Here, by employing three different metals with distinct attractive and repulsive parametrizations of the Gupta potential, we show that the structures of the lowest-energy isomers, and hence some of the existing controversy, is a sensitive function of potential form.

In the following section the Gupta potential is presented. In Sec. III we detail the symbiotic search for the low-energy isomers. In Sec. IV we present the geometries, structure factors, and energy distributions of the lowest-energy isomers found. Results are compared with other calculations and with the existing experimental data. In Sec. V we discuss the relevance of this work in resolving some of the ordered/disordered controversy. Specifically, in light of the findings presented here, in conjunction with *ab initio* and experimental x-ray powder diffraction data, we conclude that certain Au nanoclusters between ~19 and 75 atoms in size are disordered in their lowest-energy configurations. Finally, we summarize the relation found between the form of the potential and the geometry of the global minimum and energy ordering of the most stable isomers.

II. THE n-BODY GUPTA POTENTIAL

The Gupta potential[19] for the metal bond is based on the second moment approximation of the electron density of states in the tight-binding model.[20,21] It contains an attractive effective band term (due to the large d-band density of states) and a short-range repulsive pair potential. It is expressed in the following form:

$$V = \frac{U_n}{2} \sum_{j=1}^{n} V_j , \tag{1}$$

$$V_j = \left[A \sum_{i(\neq j)=1}^{n} \exp[-p(r_{ij}/r_{0n}-1)] - \left(\sum_{i(\neq j)=1}^{n} \exp[-2q(r_{ij}/r_{0n}-1)] \right)^{1/2} \right]. \tag{2}$$

The first term in the square brackets of Eq. (2) represents the Born-Mayer repulsion and the second the n-body cohesive energy of the metallic bonding. The parameters p and q depend on the atom type and are obtained by fitting to the bulk equilibrium distance and elastic constants.[20] The values of A were obtained by minimizing the bulk fcc cohesive energy. Table I lists the values of the parameters for the metals investigated in this work. Note that r_{0n} and U_n are functions of the number of atoms n in the cluster. In all of the results presented here, except in the comparison of structure factors

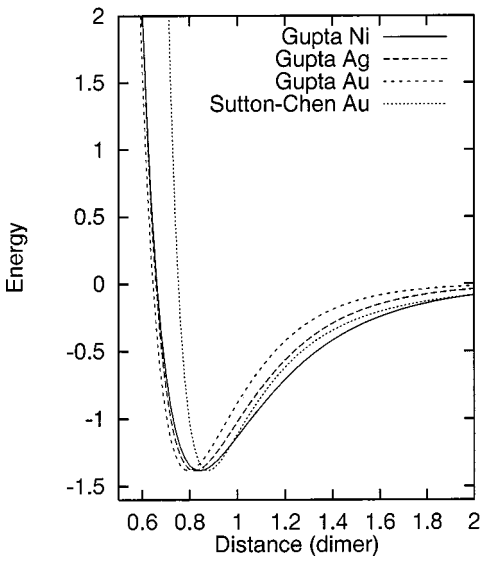

FIG. 1. The Gupta potential in reduced units for the dimer of the three different metals, Au, Ag, and Ni. Note the differences in the range of the potentials. For comparison, the Sutton-Chen potential for Au is plotted with its minimum normalized to that of Gupta.

with experiment, reduced units are used in which $r_{0n}=1.00$ and $U_n=1.00$. All energies listed in this work are for the entire cluster.

The potential was originally derived for modeling transition metals where the d band is most important but it has also been shown to be valid for noble metals, where s-d hybridization would require including higher moments, by simply extending the range of the potential.[22] This potential has been used extensively in modeling transition and noble metal clusters[9,23,24] as well as bulk metals.[25] An n-body Gupta-like potential has also been recently parametrized for alkali metal clusters.[26]

The dependence of the Gupta potential on atomic separation for the dimer molecule of the three different metals considered here is shown in Fig. 1. For comparison, the depths of the three potentials have been scaled to the same value. The range of the attractive interaction is defined by the parameter q and the repulsive core by the parameter p. Gold has the shortest range (largest value of q), and nickel the longest (smallest value of q). The repulsive core, in reduced units, is similar for all three metals. For later reference, we have also plotted the depth normalized Sutton-Chen potential for Au, with the parameters obtained from Ref. 7.

III. THE SEARCH FOR THE LOW-ENERGY ISOMERS

The potential energy surface of the cluster defined by the Gupta potential is complex and becomes more so the shorter the range of the potential. The number of local minima increases rapidly with the size of the cluster and the attraction basins of the minima have different widths. Finding the lowest-energy isomers is thus a difficult task requiring an efficient, global optimization approach.

Genetic algorithms are global optimization routines based on the analogy of evolution through natural (fitness based) selection in nature. They have been successfully applied to the cluster optimization problem[13,27–29] and have been shown

to be more efficient than simulated annealing, using either Monte Carlo or molecular dynamics, in finding the lowest-energy minima.[27,30–32]

For large clusters, we have demonstrated that the genetic algorithm can be substantially improved by taking advantage of a peculiarity of the fitness function (the binding energy) directing the selection process. Nearest neighbor atom coordinates are tightly coupled through the fitness function. Evolving in cells and then forming and evolving a symbiosis of the results is substantially more efficient than evolving the whole cluster as a single system.[13] This is particularly true if a complete set of low-energy minima is sought and not just the global minimum.[13]

Because of the stochastic nature of the moves on the potential energy surface, the symbiotic algorithm, and evolutive algorithms in general, avoid entrapment in high-energy local minima, providing a more global search. The price paid for not conforming to the forces is the loss of dynamical information. However, the efficiency of the symbiotic approach permits an exhaustive survey of a large portion of the low-energy minima and saddle points, thus allowing the prominent features on the potential energy landscape to be mapped out and thereby providing substantial insight into the dynamics.[13,33]

The symbiotic algorithm begins by generating a random initial configuration of the coordinates of the n atoms of the cluster within a sphere of radius $1.62\times(n/75)^{1/3}$. This radius, determined heuristically, gave an initial volume most efficient for the optimization process. However, the cluster was allowed to expand or contract out of this volume. A template genetic string for this configuration, with the genes corresponding to the Carteasian coordinates of the atoms, was encoded in 8 bit Gray binary form. A spherical cell was then defined of radius 0.68 (containing on average $m=8$ atoms) centered on the point in physical space of the first atom appearing in the genetic string. Variables corresponding to the coordinates of the atoms which lay within this cell were mutually optimized using the standard evolutive technique[34] of mutation and crossover with selection based on the cell fitness function

$$V_c=\frac{U_n}{2}\sum_{l=1}^{m} V_l, \tag{3}$$

where the sum on l is only over the m atoms within the cell and V_l is as defined in Eq. (2).

The $n-m$ atoms outside the cell are fixed but provide an energy contribution to the cell which depends on both the cell configuration and the configuration of the rest of the cluster. The atom coordinates within the cell were evolved until the best energy for the cell did not change in seven consecutive generations. At this point a symbiosis was formed between the cell and the rest of the cluster by updating the template genetic string with the optimized cell coordinates if this action gave a lower energy to the entire cluster as determined by the fitness function for the whole cluster, Eq. (1).

The next cell was similarly defined, centered on the second atom appearing in the genetic string and the evolutive and symbiotic process repeated in this manner until the best energy for the entire cluster did not change in 15 consecutive symbiotic events. At this point the entire cluster was locally optimized by applying a conjugate gradient minimization. For each cluster size of each element, we carried out 50 000 such symbiotic optimizations for the smaller clusters and 80 000 for the two largest ones, each optimization beginning from a distinct random initial configuration.

IV. RESULTS

Unlike in most other implementations of the genetic algorithm, the symbiotic algorithm does not just fixate on finding the global minimum but provides a complete distribution of the lowest-energy minima. Figure 2 shows, for the three metals, the distributions in energy of the low-energy stationary points found, in 50 000 runs of the symbiotic algorithm for the cluster size of 38 atoms, and in 80 000 runs for the cluster sizes of 55 and 75 atoms. For the larger clusters, the symbiotic algorithm found more than 10 000 stationary points but only the 100 lowest-energy ones are plotted in Fig. 2. The separation in energy of the low-energy states, in particular, that between the ground state and the other isomers, appears to have a direct relation to the range of the potential (large for nickel and small for gold). Also, in general, the encounter frequency of the global minimum decreases with both a decreasing range of the potential and increase in cluster size, indicative of both an increase in the number of local minima and a decrease in the attraction basin width of the global minimum. The exception is Au_{38} which appears to have a large attraction basin width for its global minimum (a disordered structure). The insets of the figures show the density of configurations in energy as a function of energy. Note that the density of states for Au is significantly larger than that for either Ag or Ni. Such trends are evident over the whole range of cluster sizes studied here. These details in the energy distribution of the low-energy isomers play a crucial role in defining the thermodynamics of the cluster, for example, on the heat capacity and the phase transition temperatures.[35] The relation between the distribution in energy of the isomers and the thermodynamics of these metal clusters will be detailed in a forthcoming article.[36]

Figure 3 presents the geometries of the three lowest-energy isomers found of each size for the different metals. For $n=6$ and $n=7$, all three metals have the same three lowest-energy isomers, and in the same order in energy. The global minima are the octahedron and the pentagonal bipyramid respectively, in agreement with results using the Sutton-Chen potential.[7,37] Differences in the ordering of the isomers for the metals (attributable, in the most part, to the differences in the attractive potential range) begin to appear at a cluster size of 12 atoms. The Ni and Ag cluster global minima are based on variants of the icosahedral structure for $n=12,13,14,19$, and 55. For Ni at $n=12,13,14$, and 19 the global minima found here with the Gupta potential are identical to those found with the Sutton-Chen potential.[7,37] At $n=13$ all three metals have the closed shell icosahedral structure, in agreement with results using the Sutton-Chen potential[7] and even with a two-body Morse potential.[38] For both Ni and Ag at $n=19$ and 38 we found the two interpenetrating icosahedra and the fcc truncated octahedron, respectively, as the lowest-energy configurations, in agreement with a study of Ni using a similar Gupta potential.[39] At n

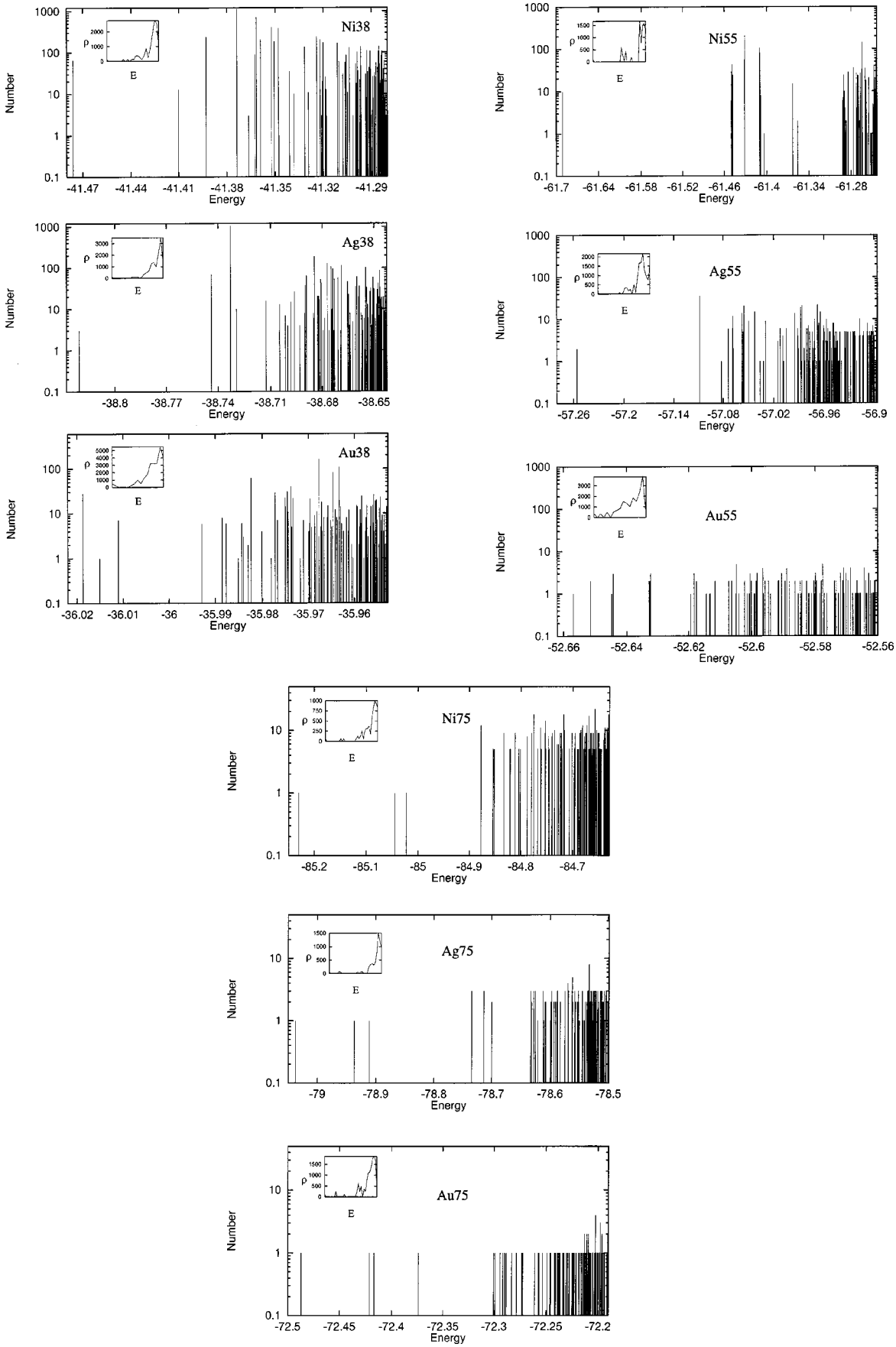

FIG. 2. Energy distribution of the 100 lowest-energy stationary points found in 50 000 (or 80 000, see text) runs of the symbiotic algorithm. The energy values are in reduced units and the number of times the point was found is plotted on a logarithmic scale on the *y* axis. The insets show the density of states in energy over the same range of energy as the corresponding distribution.

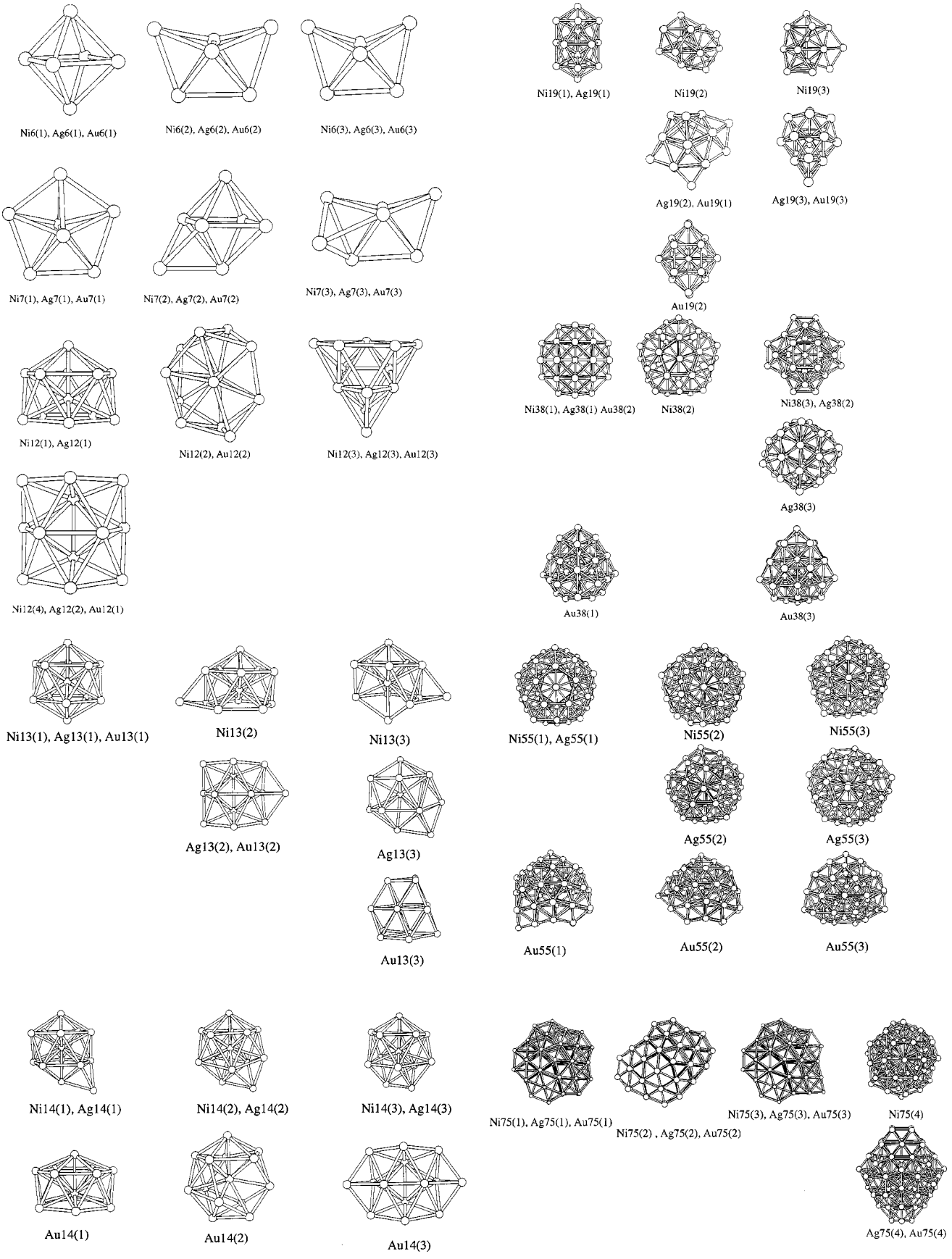

FIG. 3. The geometry of the three lowest-energy isomers found for each cluster size. The number in parentheses is the isomer number, with the lowest-energy isomers having the lowest number label.

$=55$, Ni and Ag take on the closed shell Mackay icosahedral structure. This closed shell structure for the global minimum has also been predicted by corrected effective medium theory[40] and by an embedded-atom method for Ni_{55} (Ref. 41) and with the Sutton-Chen potential for Ni_{55} and Ag_{55}.[7] For $n=75$, Ni and Ag both take on the Marks decahedral geometry. This, again, is in agreement with searches using the Sutton-Chen potential.[7]

The situation is significantly different for Au. The global minimum of Au_{13} has the icosahedral structure but for $n=12$ and 14 the global minimum is based on a hexagonal motif. Au_{19} has a unique structure for its global minimum, not easily classified. In fact, the distribution of interatomic distances for this cluster (not shown here) exemplifies a disordered structure. Au_{38} shows a disordered structure with, however, one plane of reflection symmetry (perpendicular to the paper in Fig. 3). In contrast, both the embedded-atom and Sutton-Chen potentials predict the fcc ground state for Au_{38}, as they do for Ni_{38} and Ag_{38}.[5,7] The global minimum and at least 360 other low-energy isomers of Au_{55} are disordered and have lower energy than the icosahedral structure. For Au_{75}, the lowest-energy structure obtained with the Gupta potential appears to be the Marks decahedral, as it is for Ag and Ni, in agreement with Sutton-Chen and the embedded-atom model, however, there are many disordered isomers of almost identical stability. Figure 3 gives one such disordered structure as the fourth isomer of Au_{75}, with however, one plane of reflection symmetry, oriented perpendicular to the page. Table II contains the corresponding energies of the isomers reported here in reduced units. The energy of the disordered structure for Au_{75}, not reported in the table, is -72.3771 and the energies for the icosahedral configurations of gold are Au_{38}: -35.9173, Au_{55}: -52.5177, and Au_{75}: -72.2021.

Figure 4 demonstrates the disordered nature of the isomers of Au_{38}, Au_{55}, and Au_{75} by comparing their distribution of interatomic distances with those obtained for the ordered geometries. Note that the icosahedral clusters of 38 and 75 atoms in size do not correspond to closed shells and therefore present considerable structural deformation, apparent in their distribution of interatomic distances.

In order to better understand the apparently anomalous structures of Au nanoclusters modeled with the Gupta potential, we have plotted the energy difference between the disordered and fcc structures for 38 atoms as a function of the parameters p and q of the Gupta potential in Fig. 5. For these calculations, the value of the parameter A of the potential has been optimized to give the lowest energy for the fcc bulk for each set of p and q values. There is, apparently, a significant window on p and q for which the disordered structure is lower in energy than the fcc. The Gupta potential parameters for Au fall within this window, however, those of Ag and Ni do not. Fitting the parameters of the Gupta potential to the repulsive core and attractive range of the Sutton-Chen potential for Au plotted in Fig. 1 (giving $p\sim12.3$, and $q\sim3.6$), and taking account of Fig. 5, indicates why the disordered states are higher in energy than the fcc configuration for the Sutton-Chen potential. However, the disordered structure for Au_{38} is a local minimum of the Sutton-Chen potential and it has an energy of only 0.08% larger than the fcc global minimum. We note that the fcc and disordered structures coexist in a narrow band of energy in both the regions labeled ''fcc'' and ''disordered'' of the p-q plane.

TABLE II. Energies (in reduced units) of the three lowest-energy stationary points found for each cluster size. The *'s mark saddle points, all others are stable minima.

	Isomer		
	1	2	3
Ni_6	−5.2968	−5.2055	−5.2006*
Ag_6	−5.2365	−5.1643	−5.1532*
Au_6	−5.1869	−5.1375	−5.1276*
Ni_7	−6.3489	−6.2861	−6.2403*
Ag_7	−6.2389	−6.1841	−6.1405
Au_7	−6.1264	−6.0904	−6.0607*
Ni_{12}	−11.7938	−11.6472	−11.6453
Ag_{12}	−11.3054	−11.2350	−11.2312
Au_{12}	−10.8049	−10.8040	−10.7966
Ni_{13}	−13.0867	−12.7764	−12.7714
Ag_{13}	−12.4724	−12.2621	−12.2577
Au_{13}	−11.7739	−11.7571	−11.7457
Ni_{14}	−14.0604	−14.0226	−14.0141*
Ag_{14}	−13.4067	−13.3735	−13.3625
Au_{14}	−12.7449	−12.7109	−12.7069
Ni_{19}	−19.7168	−19.5278	−19.5255
Ag_{19}	−18.6212	−18.5614	−18.5591
Au_{19}	−17.5617	−17.5586	−17.5536
Ni_{38}	−41.4760	−41.4102	−41.3928
Ag_{38}	−38.8207	−38.7438	−38.7329
Au_{38}	−36.0187	−36.0151	−36.0110
Ni_{55}	−61.6910	−61.4498	−61.4496
Ag_{55}	−57.2557	−57.1084	−57.0822
Au_{55}	−52.6569	−52.6515	−52.6448
Ni_{75}	−85.2305	−85.0454	−85.0224
Ag_{75}	−79.0378	−78.9368	−78.9112
Au_{75}	−72.4872	−72.4213	−72.4169

Figure 5 also shows a region in the p-q plane (which we have labeled the ''transition'' region) in which neither the disordered nor the fcc structures are stable. The stable configurations in this interesting region appear to be spatially fixed accumulations of dimers and trimers. These configurations cannot be called a gas in the usual sense because the dimers and trimers maintain their spatial relationships even at nonzero temperature. An article describing the characteristics of the stable configurations in this region is under preparation.[42]

Comparing the encounter frequencies of the disordered and ordered isomers of Au (obtained by identifying the geometries of the minima in the energy distributions of Fig. 2), and assuming that the attraction basins in coordinate space as seen by the symbiotic algorithm are related to the real attraction basins in phase space, the disordered structures would be the most probable products of cluster condensation from the gas or liquid phase. We have verified that these structures are also the most stable at finite temperatures by comparing the free energy of the disordered and crystalline structures as a function of temperature.[10] We have also confirmed the stability and energy ordering of the disordered states with respect to the crystalline states using DFT-LDA for those sizes

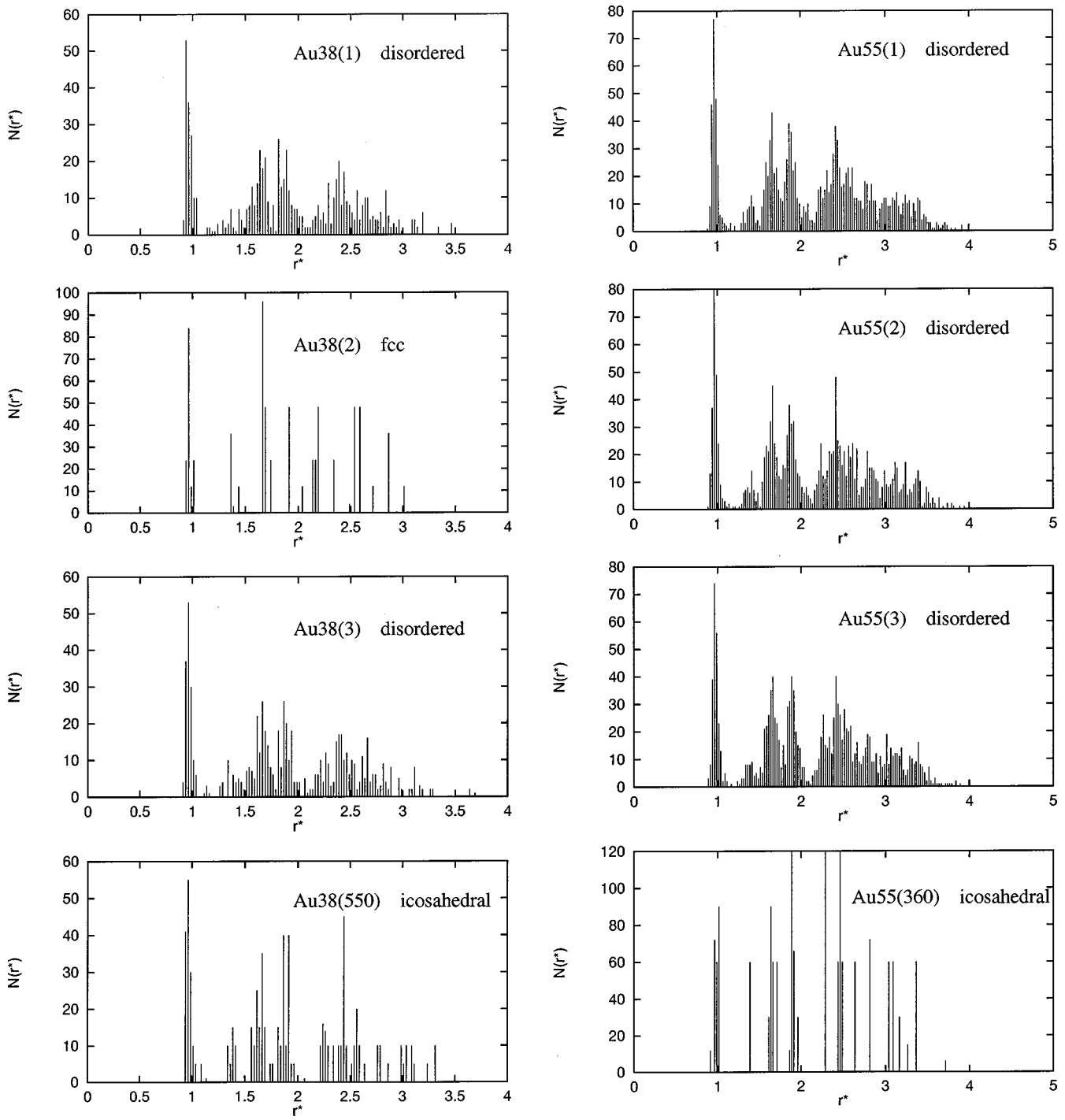

FIG. 4. The distribution of interatomic distances $N(r^*)$ (where $r^* = r_{ij}/r_{0n}$) for the disordered and ordered isomers of Au clusters of size 38, 55, and 75 atoms. The number in parentheses is the isomer number.

investigated here in which disordered states are abundant, $n = 38$, 55, and 75 (Ref. 6). In fact, although at the cluster size of 75 Au atoms, the Gupta potential predicts the Marks decahedral structure to be of lower energy than the disordered state, density functional theory predicts the disordered states to be lower.[43]

To provide a basis for comparison of the structures found here with future experiments, the structure factors corresponding to each of the geometrical configurations listed in Fig. 3 are given in Fig. 6. They were calculated according to

$$I(s) = \sum_{i,j=1}^{n} f_i f_j \frac{\sin(2\pi s r_{ij})}{2\pi s r_{ij}}, \tag{4}$$

with $s = 2\sin\theta/\lambda$, where, in experiment, θ and λ are the angle and wavelength of the incident x rays. r_{ij} is the distance in reduced units between atoms i and j in the cluster. The atomic scattering factors f_i and f_j were given the value 1.0 and no background or scaling factors have been applied. These structure factors provide a characterization of the clusters local structure which is relatively independent of size

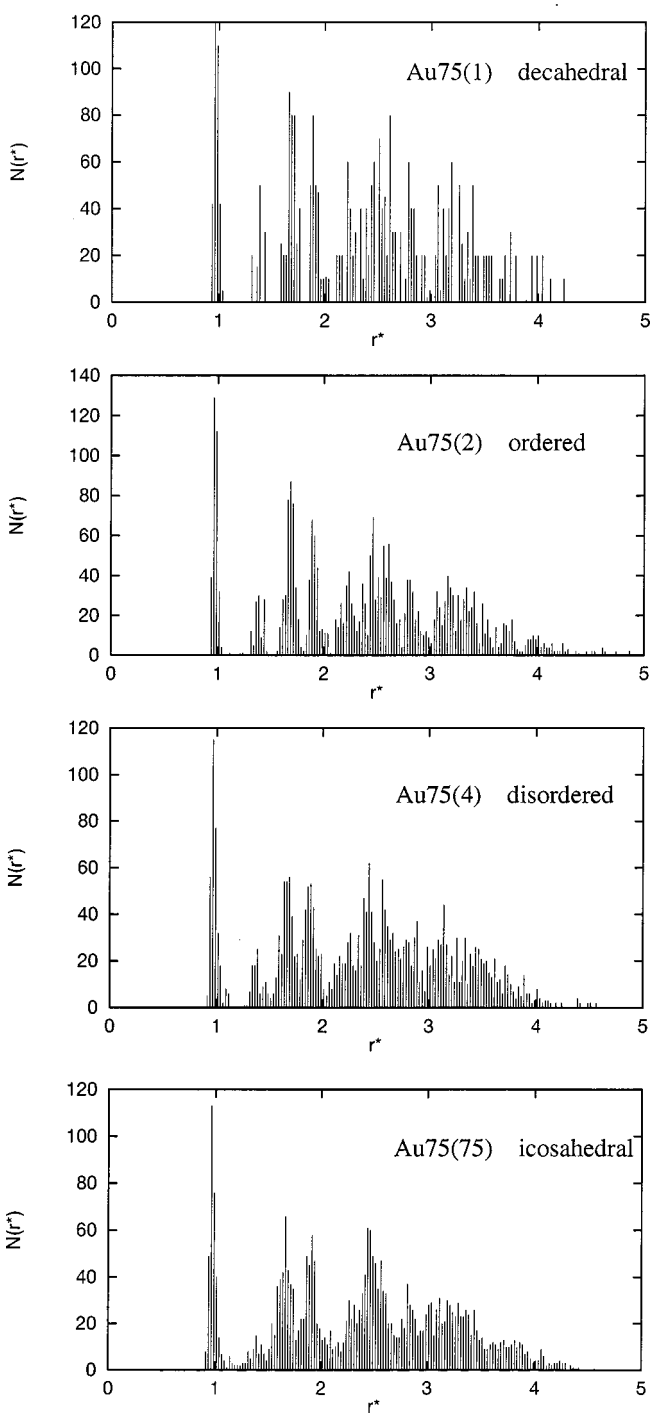

FIG. 4. (*Continued*).

and morphology. For example, the two disordered configurations presented for Au_{38} show very similar structure factors. These also compare with the disordered structure factors of Au_{55} and the disordered fourth isomer of Au_{75}.

The experimental powder x-ray structure factors obtained from mass selected samples[1,5] are given in Fig. 7 for comparison with our results on Au_{38} and Au_{75}. For appropriate comparison with experiment, the real distances were estimated using DFT-LDA data obtained for these clusters[6] and an exponential damping factor of form $\exp(-Bs^2/2)$ was included to account for thermal effects.[5] The value of B appears to be relatively independent of cluster size[5] and was

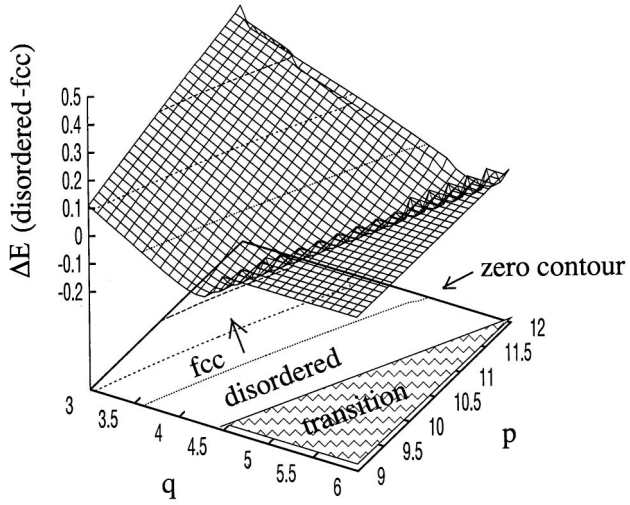

FIG. 5. A three-dimensional plot with contour lines of the energy difference (disordered-fcc) for the optimized cluster configurations of 38 atoms as a function of the parameters p and q of the Gupta potential. Note that the disordered structure is the most stable for a significant window in p and q beginning at the zero contour. The contour lines begin at zero and increment upwards by $+0.1$ in energy in moving towards the upper left of the figure. The regions of the q-p plane labeled ''disordered'' and ''fcc'' correspond to regions where the disordered and fcc structures are the global minimum, respectively. See text for an explanation of the ''transition'' region.

given the value 0.013 which was determined in Ref. 5 by fitting various simulated structure factors to the experimental spectrum of the 146-atom cluster. In distinction to the conclusions presented in Refs. 1 and 5 we suggest that the low-energy disordered structures found here reproduce the experimental spectra as well or better than any of the ordered structures. Clearly, a more appropriate comparison with experiment would be a sum over the structure factors of the lowest-energy isomers, weighted by the structures attraction basin widths and free energies. In view of the results presented here, the disordered structures would be assigned the largest weights for Au nanoclusters between ~ 19 and 75 atoms in size.

V. CONCLUSIONS

We have searched the Gupta potential energy surface of small metal nanoclusters using a global and efficient symbiotic algorithm. Disordered structures were found as the lowest-energy minima for a range of cluster sizes extending from ~ 19 to 75 atoms. These results represent the most exhaustive searches with such a potential to date that we are aware of.

The effect of the form of the potential on the geometry of the cluster global minimum and on the energy ordering of the low-energy isomers was investigated. The ordering of the isomers in energy begins to depart for the different metals around $n=12$. As the repulsive parameter p for the three metals was similar in magnitude, this can be attributed, in most part, to the different attractive ranges of the potentials. Ni and Ag clusters prefer the icosahedral structure except at $n=38$ and 75 for which the fcc and decahedral structures,

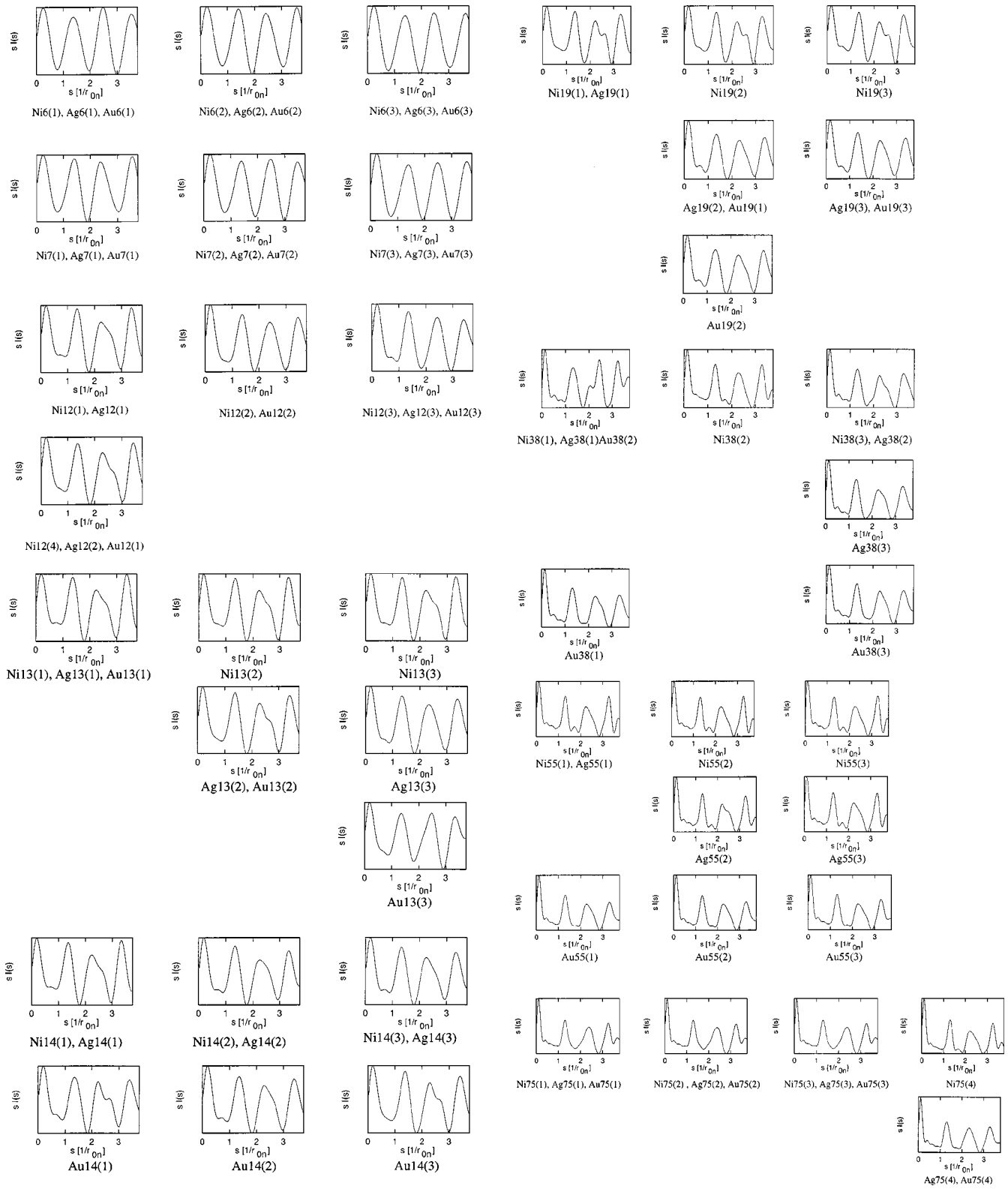

FIG. 6. The structure factors of the three lowest-energy isomers of each cluster size. These spectra were obtained using the geometries given in Fig. 3. See text for details.

respectively, have the lowest energy. Au clusters show preference for the hexagonal structure at $n=12$ and 14 and for disordered structures at $n=19$, 38, and 55. The lowest-energy Au structure is Marks decahedral at 75 atoms but there are many disordered isomers of similar energy.

For a cluster of 38 atoms, we have studied in detail how the energy difference between the disordered and fcc structures depends on the values of the potential parameters. We found a region in the p-q (repulsive core–attractive range) space of the Gupta potential where disordered structures are favored. The parameters of the Gupta potential for Au lie within this region, but those of Ni and Ag do not. The form

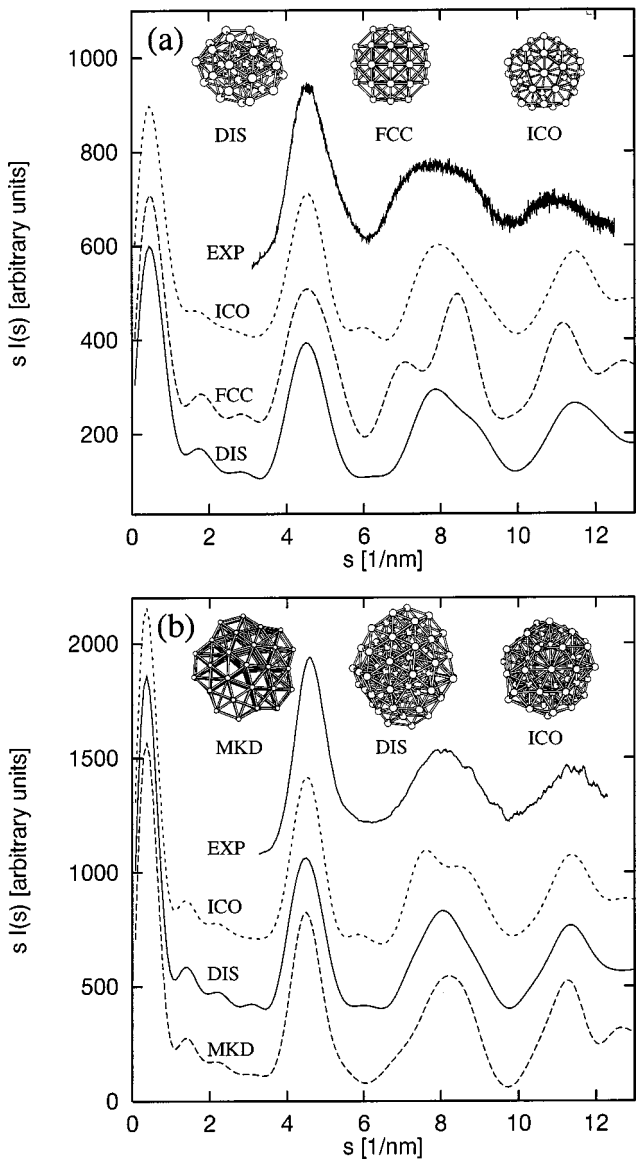

FIG. 7. Comparison of the experimental structure factors (Refs. 1 and 5) for Au_{38} (a) and Au_{75} (b) with those determined here using Eq. (4) and including a thermal damping factor (see text). Real distances have been estimated using DFT-LDA calculations. The solid line is for the disordered state, the dashed line for the fcc structure, and the dot-dashed line for the icosahedral structure. The reflection planes of symmetry of the disordered clusters have been rotated out of the viewing direction to emphasize the disordered nature of these structures.

of the Sutton-Chen potential for Au is such that its core-range combination also does not lie within this region. The structure of the global minimum and that of the low-energy isomers of small metal nanoclusters is thus a sensitive function of the form of the potential.

Another interesting region in the p-q plane (small p and large q) was found where neither the disordered nor fcc structures are stable. The stable configurations here appear to be accumulations of dimers and trimers with definite spatial relation. This information will be the subject of a following article.

The encounter frequencies of the stable configurations found in 50 000 (or 80 000) distinct runs were tabulated and related to the width of their attraction basins. The difference in energy between the global minimum and the other isomers, and the density in energy of stable states near the global minimum, were shown also to be a function principally of the attractive range of the potential for these metals. The shorter the range, the higher the density of states and the smaller the energy gap between the global minimum and the higher-energy isomers. The details of this relation between the distribution of minima in energy and the thermodynamics of metal nanoclusters is left to a forthcoming article.

The disordered states of Au clusters of size 19, 38, 55, and 75 atoms have the largest attraction basins, and, combining this with the fact that they are the most stable of all the configurations at finite temperature, we predict that they would be the most probable result of cluster condensation from the gas or liquid. Supporting this prediction, we cited the results of density functional calculations and the fact that, at least qualitatively, the experimental structure factors for Au_{38} and Au_{75} appear most like those generated from the disordered states found here than those from the ordered states. We emphasize that this is in contrast to the conclusions in the existing literature on gold nanoclusters.[1,5] We suggest that previous conclusions drawn from comparing the experimental data with theoretical predictions were biased because of lack of a complete set of low-energy disordered configurations. The disordered states were not previously isolated because prior searches fixated on finding the global minimum and subtle differences in the form of the potential led to slightly higher energies for the disordered structures. We therefore suggest that the ordered/disordered controversy concerning the structure of metal nanoclusters resulted from the different repulsive core–attractive range relations of the various potentials used. Further attention should thus be paid to improving the potential model representations of the metal bond and the delineation of subtle differences in these on the predictions of the geometries of the low-energy minima of metal nanoclusters. Finally, it should be mentioned that many other Au clusters between 19 and 75 atoms are also expected to be disordered. Work on verifying this, and determining the effect of the passivation layer on the cluster structures of the experimental samples, although assumed to be small, is now under investigation.[44]

ACKNOWLEDGMENTS

The financial support of DGAPA-UNAM Grant No. IN101297, and CONACYT Grant No. 25083E, as well as the computational support of DGSCA-UNAM Supercomputing Center are gratefully acknowledged.

[1] T. G. Schaaff, M. N. Shafigullin, J. T. Khoury, I. Vezmar, R. L. Whetten, W. G. Cullen, P. N. First, C. Gutiérrez-Wing, J. Ascensio, and M. José-Yacamán, J. Phys. Chem. B **101**, 7885 (1997).
[2] R. P. Andres, T. Bein, M. Dorogi, S. Feng, J. I. Henderson, C. P. Kubiak, W. Mahoney, R. G. Osifchin, and R. Reifenberger, Science **272**, 1323 (1996).
[3] A. P. Alivisatos, Science **271**, 933 (1996).
[4] C. S. Lent and P. D. Tougaw, Proc. IEEE **85**, 541 (1997).
[5] C. L. Cleveland, U. Landman, T. G. Schaaff, M. N. Shafigullin, P. W. Stephens, and R. L. Whetten, Phys. Rev. Lett. **79**, 1873 (1997); C. L. Cleveland, U. Landman, M. N. Shafigullin, P. W. Stephens, and R. L. Whetten, Z. Phys. D **40**, 503 (1997).
[6] I. L. Garzón, K. Michaelian, M. R. Beltrán, A. Posada-Amarillas, P. Ordejón, E. Artacho, D. Sánchez-Portal, and J. M. Soler, Phys. Rev. Lett. **81**, 1600 (1998).
[7] J. P. K. Doye and D. J. Wales, New J. Chem. **22**, 733 (1998).
[8] M. M. Alvarez, J. T. Khoury, T. G. Schaaff, M. Shafigullin, I. Vezmar, and R. L. Whetten, Chem. Phys. Lett. **266**, 91 (1997).
[9] I. L. Garzón and A. Posada-Amarillas, Phys. Rev. B **54**, 11 796 (1996).
[10] I. L. Garzón, K. Michaelian, M. R. Beltrán, A. Posada-Amarillas, P. Ordejón, E. Artacho, D. Sánchez-Portal, and J. M. Soler (unpublished).
[11] S. H. Yang, D. A. Drabold, J. B. Adams, P. Ordejón, and K. Glassford, J. Phys.: Condens. Matter **9**, L39 (1997).
[12] A. Sachdev R. I. Masel, and J. B. Adams, Catal. Lett. **15**, 57 (1992).
[13] K. Michaelian, Chem. Phys. Lett. **293**, 202 (1998).
[14] P. A. Braier, R. S. Berry, and D. J. Wales, J. Chem. Phys. **93**, 8745 (1990).
[15] J. P. K. Doye and D. J. Wales, J. Phys. B **29**, 4859 (1996); J. Chem. Soc., Faraday Trans. **93**, 4233 (1997).
[16] C. Rey and L. J. Gallego, Phys. Rev. E **53**, 2480 (1996).
[17] C. Rey, J. Garcia-Rodeja, L. J. Gallego, and M. J. Grimson, Phys. Rev. E **57**, 4420 (1998).
[18] I. G. Kaplan, *Theory of Intermolecular Interactions* (Elsevier, Amsterdam, 1986).
[19] R. P. Gupta, Phys. Rev. B **23**, 6265 (1981).
[20] V. Rosato, M. Guillope, and B. Legrand, Philos. Mag. A **50**, 321 (1989).
[21] A. P. Sutton, *Electronic Structure of Materials* (Oxford University Press, New York, 1993).
[22] F. Cleri and V. Rosato, Phys. Rev. B **48**, 22 (1993).
[23] C. Rey, L. J. Gallego, J. Garcia-Rodeja, J. A. Alonso, and M. P. Iñiguey, Phys. Rev. B **48**, 8253 (1993).
[24] A. Posada-Amarillas and I. L. Garzón, Phys. Rev. B **54**, 10 362 (1996).
[25] A. Posada-Amarillas and I. L. Garzón, Phys. Rev. B **53**, 8363 (1996).
[26] Y. Li, E. Blaisten-Barojas, and D. A. Papaconstantopoulos, Phys. Rev. B **57**, 15 519 (1998).
[27] R. S. Judson, M. E. Colvin, J. C. Meza, A. Huffer, and D. Gutierrez, Int. J. Quantum Chem. **44**, 277 (1992).
[28] D. M. Deaven and K. M. Ho, Phys. Rev. Lett. **75**, 288 (1995).
[29] D. M. Deaven, N. Tit, J. R. Morris, and K. M. Ho, Chem. Phys. Lett. **256**, 288 (1996).
[30] B. Hartke, J. Phys. Chem. **97**, 9973 (1993).
[31] Y. Zeiri, Phys. Rev. E **51**, R2769 (1995).
[32] Y. Zeiri, Comput. Phys. Commun. **103**, 28 (1997).
[33] D. J. Wales, Science **271**, 925 (1996).
[34] K. Michaelian, Am. J. Phys. **66**, 231 (1998).
[35] M. Moseler, J. Nordiek, and H. Haberland (unpublished).
[36] K. Michaelian, I. L. Garzón, A. Tamez (unpublished).
[37] S. K. Nayak, S. N. Khanna, B. K. Rao, and P. Jena, J. Chem. Phys. **101**, 1072 (1997).
[38] W. Hu, L. M. Mei, and H. Li, Solid State Commun. **100**, 129 (1996).
[39] F. Aguilera-Granja, S. Bouarab, M. J. López, A. Vega, J. M. Montejano-Carrizales, M. P. Iniguez, and J. A. Alonso, Phys. Rev. B **57**, 12 469 (1998).
[40] T. L. Wetzel and A. E. DePristo, J. Chem. Phys. **105**, 572 (1996).
[41] J. Jellinek, in *Metal-Ligand Interactions*, edited by N. Russo and D. R. Salahub (Kluwer Academic, Dordrecht, 1996), p. 325.
[42] K. Michaelian and I. L. Garzón (unpublished).
[43] J. M. Soler, M. Beltrán, K. Michaelian, I. L. Garzón, P. Ordejón, D. Sánchez-Portal, and E. Artacho (unpublished).
[44] K. Michaelian and I. L. Garzón (unpublished).